ChemComm

Accepted Manuscript

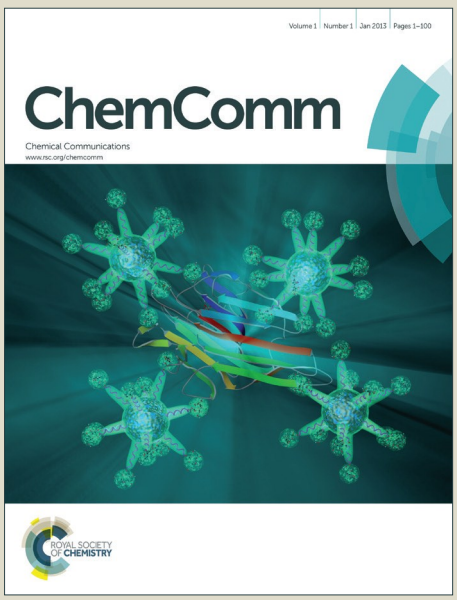

ROYAL SOCIETY OF CHEMISTRY

www.rsc.org/chemcomm

ChemComm

COMMUNICATION

Nanogrooves-guided Slot-die Coating for Highly Ordered Polymer Films and High-mobility Transistors

Received 00th January 20xx,
Accepted 00th January 20xx

DOI: 10.1039/x0xx00000x

www.rsc.org/

Aung Ko Ko Kyaw,*[a] Lim Siew Lay,[a] Goh Wei Peng,[a] Jiang Changyun[a] and Zhang Jie*[a]

Nanogrooves-guided slot-die coating technique is developed to manipulate the alignment of polymer chains within a short processing time. A combination of directional movement of slot-die and uniaxial nanogrooves on the substrate for the unidirectional flow of solution suppresses the multiple degrees of conformational freedom, resulting in long-range oriented polymer films and high field effect mobility of ~5 $cm^2V^{-1}s^{-1}$.

Semiconducting polymers have a great potential to achieve low-cost and large-area fabrication of flexible electronic devices for display, sensing, artificial intelligence and healthcare applications.[1] However, the random packing of polymer chains and the disordered nature of the polymer matrix typically result in low carrier mobility (10^{-5}-10^{-2} $cm^2V^{-1}s^{-1}$), limiting their device performance and the further development of integrated circuits in which high switching speed is required. A long-range alignment of polymer chains in a thin film by solution-process remains challenging in polymer electronics research mainly due to the tendency for entanglement of polymer fibre, stochastic nucleation and fluid dynamics in wet film deposition and drying mechanism.

Several strategies have been proposed to enforce ordered structures within the polymer fibres and to increase the mobility of polymer semiconductors. Both molecular designs[2] and solution processing techniques such as surface-induced molecular ordering,[3] mechanical rubbing[4] and directional film deposition methods[5] have been proposed to improve the charge transport through ordered polymer chains. With a synergic effort, the mobility of field effect transistors (FETs) in a range of 1-10 $cm^2V^{-1}s^{-1}$ has been achieved, exceeding those of amorphous silicon.[2a, 2b, 6] Despite this improvement, the mobility of polymer based transistors is still lower than that of the crystalline small molecule based counterparts.[7] In fact, semiconducting polymers possess better film forming capability and mechanical property compared to small molecules, resulting in improved flexibility and large-area uniformity.

Recently, a semiconducting polymer with field effect mobility up to 21 $cm^2V^{-1}s^{-1}$ and intrinsic mobility of 47 $cm^2V^{-1}s^{-1}$, which is comparable to that of small molecule single crystals, was reported using capillary action mediated film deposition in a sandwich tunnel structure.[8] Such unprecedented mobility was attributed to self-assembly of macroscopically aligned polymer films. The mobility, however, is highly dependent on the transistor location: mobility is high where the aligned nanocrystalline polymer film exists and is not consistent throughout the entire substrate. Moreover, this method and other slow evaporation methods for slow growth of polymer film require a significantly long processing time during film deposition (5 h or more),[2b, 8] preventing from rapid and uniform production of large-area distributed products. Hence, the development of appropriate processing techniques without sacrificing high throughput and scalability becomes an essential requirement for the fabrication of long-range orientated semiconducting polymer films.

Slot-die coating is a well-suited method for production of large-area film with high throughput. It has been adopted in the fields of lacquer and paint industries due to its reliable, accurate and reproducible thin film production. More importantly, this method saves raw materials and has a good control over film thickness, uniformity and batch-to-batch consistency. Slot-die coating has been demonstrated for organic solar cells, polymer light-emitting diodes, electrochromic devices and organic thin film transistors, in addition to barrier film coatings for medical and food packaging manufacturing.[9] In this communication, we introduce a nanogrooves-guided slot-die coating technique, which is different from traditional slot-die coating, to further improve the control and guidance in polymer chain alignment. A combination of directional movement of slot-die and uniaxial nanogrooves on the substrate for the unidirectional flow of solution suppresses the multiple degrees of conformational freedom, resulting in long-range oriented polymer films and high FET mobility of ~5 $cm^2V^{-1}s^{-1}$ without sacrificing high throughput and scalability.

The schematic diagram of the slot-die coating process employed in this study is illustrated in Fig. S1 (Supplementary Information). The substrates are fixed on a temperature-controlled vacuum chuck. A small volume of polymer solution is coated onto the substrate by a slot-die with different wet-film thickness (slot-die gap) ranging from 15 µm to 200 µm. The moving speed of the slot-die is controlled by a linear motor. A uniform thin film can be coated on both rigid and flexible large-area substrates such as silicon, glass and polyethylene terephthalate (PET) by this slot-die coating method. A donor−acceptor copolymer, poly[4-(4,4-

[a] *Institute of Materials Research and Engineering (A*STAR), 2 Fusionopolis Way, Singapore 138634. Email: kyawakk@imre.a-star.edu.sg, zhangj@imre.a-star.edu.sg*

† Electronic Supplementary Information (ESI) available: Details of slot-die coating process, characteristics of transistors. See DOI: 10.1039/x0xx00000x

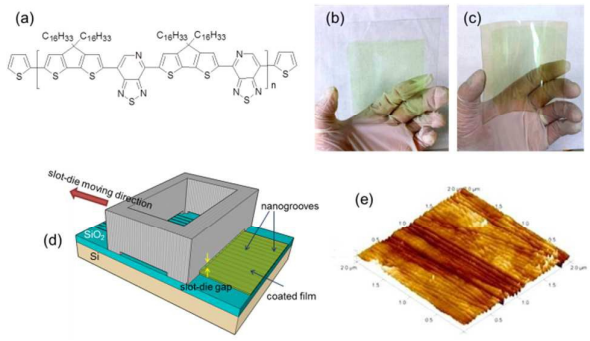

Fig. 1. The molecular structure of PCDTPT (a). The photograph of PCDTPT film coated by slot-die coating on a glass substrate (b) and a flexible ITO-coated-PET substrate (c) with an area of 10 cm x 10 cm. The illustration of nanogrooves-guided slot-die coating on a silicon substrate with thermally grown SiO_2 layer (d). The 3D AFM image of the nanogrooves fabricated on the SiO_2/Si substrate (e). The scan size is 2 µm x 2 µm.

dihexadecyl-4Hcyclopenta[1,2-b:5,4-b]dithiophen-2-yl)-alt[1,2,5]thiadiazolo [3,4c] pyridine] (PCDTPT), whose molecular structure is shown in Fig. 1a, was coated on a glass substrate and a flexible ITO-coated-PET substrate, with both having an area of 10 cm x 10 cm. The coated glass and flexible samples are shown in Fig. 1b and 1c, respectively. The moving speed of the slot-die influences the thickness and uniformity of the coated film (Fig. S2, Supplementary Information). The PCDTPT film with uniform dry-film thickness of 20 nm was obtained from a solution concentration of 4 mg/mL in chlorobenzene, a slot-die gap of 90 µm (wet-film thickness) and a relatively fast moving speed of 3 mm/s. This demonstrates that slot-die coating provides a large-area uniform coating within a short processing time.

Besides its potential for large-area production with high throughput, slot-die coating combined with an appropriate guiding channel (nanogrooves) ensures the unidirectional flow of solution for the confinement of polymer fibres in specific orientation, offering a better macroscopic alignment in polymer chains compared to non-directional coating such as spin coating. To demonstrate this concept, we deposited PCDTPT film on heavily n-doped silicon substrates with 2000 Å-thick-SiO_2 by nanogrooves-guided slot-die coating, as illustrated in Fig. 1d. First, uniaxial nanogrooves were fabricated on the substrates by scratching the SiO_2 surface with diamond lapping films. Since the nanogrooves obtained by this method are very fine, no visible scratches were spotted on the surface. However, uniaxial nanogrooves with a depth of ~ 1-2 nm were clearly seen in atomic force microscopy (AFM) images (Fig. 1e and S3 in the Supplementary Information). Moreover, a parallel flow of liquid in the same orientation as the scratching direction was observed when the substrate was sprayed with deionized water and held in a vertical position (Fig. S4, Supplementary Information), suggesting that liquid (solution) can be directed along the nanogrooves while it is flowing on the substrate, especially with the additional guidance created by slot-die coating. Therefore, these aligned nanogrooves are made parallel to the direction of slot-die coating in subsequent coating process, in order to serve as guiding channels for unidirectional solution flow and to promote polymer chain alignment during coating. It is worth mentioning that because the nanogrooves are very shallow, the change in thickness of SiO_2 layer is very subtle (less than 1%). Hence, a similar capacitance of ~ 1.7×10^{-8} F/cm^2 was measured for both substrates with and without nanogrooves. The fabrication of nanogrooves using this method is also applicable to other substrates (for e.g. glass and ITO) but it probably may damage the polymeric dielectric film such as poly-4-vinyl phenol.

Since the nanogrooves are very shallow, they may not support the alignment of polymer up to the top surface. Nevertheless, they can induce alignment in the first few monolayers at the buried interface where the charge transport mainly takes place in FET. To verify this, cross-polarized optical microscopic imaging and tapping-mode AFM were, therefore, conducted at the bottom surface of the polymer film (See Supplementary Information for experimental details). Although the optical microscopic images under bright field do not exhibit significant difference between the films (Fig. S5, Supplementary Information), the cross-polarized optical microscopic images clearly elucidate the role of directional and guided solution flow during coating (Fig. 2a and 2b). The cross-polarized image of the spin-coated film shows only irregular texture, indicating that polymer fibres are in random orientation. In contrast, a long-range and highly-ordered crystallographic alignment can be clearly seen in the film deposited by nanogrooves-guided slot-die coating.

We observed a similar trend in the alignment of polymer fibres in AFM images (Fig. 2c and 2d). The polymer fibre structures are completely random in the spin-coated film whereas highly ordered fibres with apparently crystalline domain can be clearly seen in the film deposited by nanogrooves-guided slot-die coating. Although a fibre width of 20-30 nm is observed in both films, the film deposited by nanogrooves-guided slot-die coating has so much longer fibre length than the one deposited by spin-coating does, resulting in fibre lengths approaching the micrometre scale. It is worth mentioning that the crystallographic alignment in both cross-polarized and AFM images corresponds to the direction of uniaxial nanogrooves on the substrate and the direction of slot-die coating, implying that the polymer solution flows in the direction of slot-die movement along the nanogrooves where the polymer chains have diffused, nucleated and grown. During spin coating, however, the solution flows radially (in multiple directions) from the centre to the edge of the substrate due to centrifugal force, providing multiple degrees of freedom for the polymer chains during nucleation, and thus preventing them from growth in an aligned manner.

Since AFM analysis is limited to the surface morphology, information about molecular packing and crystallinity were investigated with X-ray diffraction (XRD) scanned in both out-of-

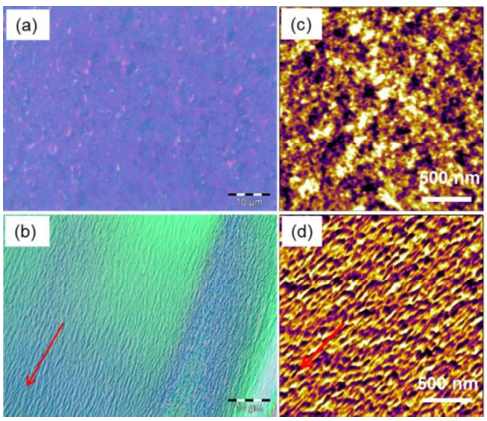

Fig. 2. The cross-polarized microscopic images (left column) and AFM images (right column) of the bottom surface of PCDTPT films deposited by spin coating (a & c) and nanogrooves-guided slot-die coating (b & d). The arrow in (b & d) represents the direction of uniaxial nanogrooves and slot-die movement.

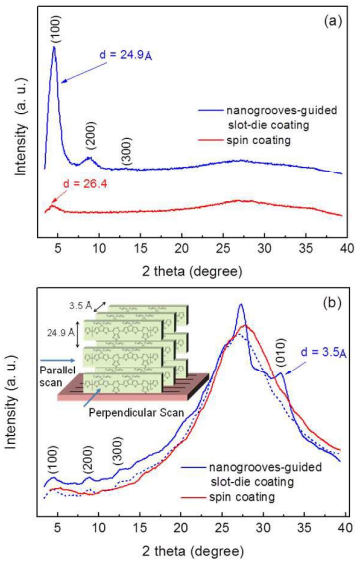

Fig. 3. Out-of-plane (a) and in-plane grazing incidence (b) XRD profile of the films deposited by nanogrooves-guided slot-die coating and spin coating. The solid line and dotted line in (b) represent the scan perpendicular and parallel to the nanogrooves, respectively. The inset illustrates preferential polymer orientations along the nanogrooves and calculated spacing between the planes.

plane and in-plane grazing incidence geometries. As shown in Fig. 3a, the out-of-plane XRD profile of the film processed by spin coating exhibits only the first order lamellar scattering which is observed as a weak peak (100) at 2θ ≈ 4.23°. In contrast, the out-of-plane XRD profile of the film deposited by nanogrooves-guided slot-die coating shows a sharp peak (100) at 2θ ≈ 4.48° as well as (200) and (300) peaks at 2θ ≈ 9° and 13.35°, respectively, from higher order reflections, indicating the long-range order in polymer film with lamella layer structures.[10] Besides the peak intensity, the shift of the (100) peak to a higher 2θ position in the film deposited by nanogrooves-guided slot-die coating suggests that *d*-spacing associated with lamella stacking decreases from 26.4 Å to 24.9 Å.

As shown in in-plane grazing incidence XRD profile which is scanned from the direction perpendicular to the nanogrooves (Fig. 3b), the peak associated with π-π stacking is observed at 2θ ≈ 32.28° (corresponding to a *d*-spacing of 3.5 Å) from the (010) plane in the film deposited by nanogrooves-guided slot-die coating. There is another peak observed at 2θ ≈ 27.31°, which is probably indicative of side chain interdigitation or another π-stacking arrangement induced by the relative sliding of polymer backbones.[10] The hump observed is most likely due to amorphous scattering from disordered polymer regions. The (010) peak, however, disappears when the film is scanned parallel to the nanogrooves although the peaks associated with lamellar stack are still remaining, implying that the polymer backbone is oriented along the nanogrooves. In contrast, scanning from both directions does not show any distinct peak in the film deposited by spin coating. From the analysis of out-of-plane and in-plane grazing incidence XRD profiles, we can deduce that the film deposited by nanogrooves-guided slot-die coating has a highly ordered edge-on orientation with a lamella layer thickness of 24.9 Å and π- π stacking distance of 3.5 Å, as illustrated in the inset of Fig. 3b. The decrease in interchain distance (higher molecular packing density) and increase in long-range order of the polymer chains are favourable for a linear backbone conformation. This enhances the

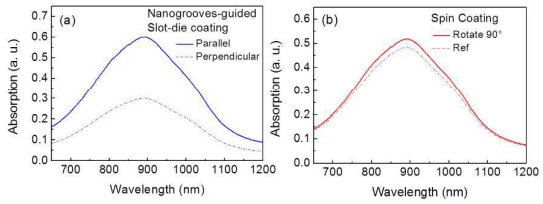

Fig. 4. Polarized Vis-NIR absorption of PCDTPT film deposited by (a) nanogrooves-guided slot-die coating and (b) spin coating

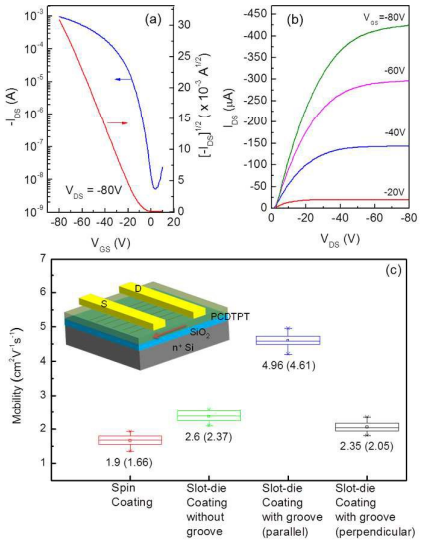

Fig. 5. The transfer (a) and output (b) characteristics of FET fabricated by nanogrooves-guided slot-die coating, showing the mobility of 4.96 $cm^2V^{-1}s^{-1}$. (c) The mobility of FETs fabricated by spin coating, conventional slot-die coating and nano-grooves-guided slot-die coating in which the channel is parallel and perpendicular to the nanogrooves. The mobility value and the value in the parentheses represent the maximum and mean values, respectively. The horizontal lines in the box denote the 25th, 50th and 75th percentile values and the error bars denote the 5th and 95th percentile values. The inset in (c) shows the device architecture in which the channel is parallel to the nanogrooves. The arrow represents the direction of slot-die movement.

p-orbital overlap over an extended conjugated system, resulting in a lowering of the interchain hopping barrier and improved charge transport characteristics.[11]

To further elucidate that the polymer backbone aligns along the nanogrooves, the polarized Vis-NIR absorption was carried out (See Supplementary Information for experimental details). In Fig. 4a the solid line and dotted line represent the absorption spectra of the PCDTPT film coated by nanogrooves-guided slot-die coating with the incident polarization parallel and perpendicular to the nanogrooves, respectively. The optical anisotropy parameter, which is determined by the ratio of the area under respective absorption curves, is about 2:1. In contrast, the optical anisotropy parameter of spin-coated film is only 1.06:1.

Using the long-range ordered polymer film deposited by nanogrooves-guided slot-die coating, we fabricated high-performance FETs. Devices were fabricated with the top-contact and bottom-gate configuration, with Au source/drain electrodes (80 nm), SiO_2 dielectric layer (200 nm) and heavily doped (n^+) Si (500 µm) gate electrode (Fig. 5c inset). The dielectric layer was treated with octadecyltrichlorosilane before polymer coating. The channel length and width are 100 µm and 500 µm, respectively. The

orientation of the channel length is parallel to the direction of solution flow and nanogrooves. In comparison, FETs with the same architecture were fabricated using PCDTPT films deposited by spin coating and conventional slot-die coating. All the polymer films deposited by various coating methods were annealed at 200°C for 8 min because annealing at this temperature gives the optimum result (Fig. S6, Supplementary Information). The coating polymer film, annealing and FET characterization were carried out in a nitrogen-filled glove box.

The transfer and output characteristics of the best FET fabricated by the nanogrooves-guided slot-die coating are shown in Fig. 5a and 5b. The electrical characteristics of the fabricated FET are very close to "ideal" behaviours which are not usually achievable in organic FET devices:[12] (1) the slope of the square root of the I_{DS} vs V_{GS} in the saturated transfer characteristics is almost linear throughout the wide range of applied gate voltages, and (2) low hysteresis is observed with multicycles of forward and reverse sweeping of the gate voltage (Fig. S7, Supplementary Information). These "near-ideal" transfer characteristics suggest the low contact resistance and the low density of shallow traps at the polymer-dielectric interface. Field effect mobility was obtained in the saturation region of transistor operation by using the equation, $I_{DS} = (W/2L)\ C_g\mu\ (V_{GS}-V_{th})^2$, where W/L is the channel width/length, C_g is the gate capacitance per unit area, V_{th} is the threshold voltage and μ is the field effect mobility. We extracted the mobility from the saturation region at low gate voltages (-20 V to -30 V), where good saturation is shown in the corresponding output curves. The FET fabricated by the nanogrooves-guided slot-die coating results in a mobility of 4.96 $cm^2V^{-1}s^{-1}$ (average mobility of 4.56 $cm^2V^{-1}s^{-1}$ from 10 devices) with high I_{on}/I_{off} ratio of 2×10^5 and a threshold voltage of -10 V. The mobility of the FET fabricated by the nanogrooves-guided slot-die coating is double the mobility of the FET fabricated by spin-coating (maximum/average mobility of 1.93/1.49 $cm^2V^{-1}s^{-1}$) or conventional slot-die coating without nanogrooves (maximum/average mobility of 2.6/2.29 $cm^2V^{-1}s^{-1}$) (Fig. 5c and Fig. S8 & S9, Supplementary Information), showing good agreement with microscopic images, AFM images and XRD profiles.

To examine the anisotropic carrier transport we also fabricated a FET in which the channel is perpendicular to the nanogrooves and slot-die coating direction. The FET shows the mobility of only 2.35 $cm^2V^{-1}s^{-1}$ (average mobility of 2.05 $cm^2V^{-1}s^{-1}$ from 10 devices) (Fig. 5c and Fig. S10, Supplementary Information), implying that the mobility along the fibre (conjugated backbone) is higher than that of perpendicular to the fibre. The charge transport anisotropy is about 2:1 which is in agreement with optical anisotropy. Thus, we attribute the higher mobility of FET fabricated by nanogrooves-guided coating to the high degree of polymer chain alignment in the long-range and enhanced intermolecular packing in the polymer film, in which anisotropic charge transport is favourable along the conjugated backbone in one-dimension with lower possibility of hopping and trapping at the grain boundaries.

In conclusion, we have demonstrated a coating strategy called nanogrooves-guided slot-die coating to fabricate highly-ordered polymer films for efficient anisotropic charge transport, without compromising on high throughput and scalability. The cross-polarized optical microscopic images and AFM images exhibit a long-range and highly-ordered crystallographic alignment in the film deposited by nanogrooves-guided slot-die coating. This crystallographic alignment is complemented by polarized absorption spectrum and XRD profiles which clearly show the higher order lamellar scatterings and increased molecular packing density. The transport along the highly-ordered conjugated chain yields a high field effect mobility of ~ 5 cm^2/V-s in the FET with configuration of top-contact and bottom-gate.

The authors are grateful to support form A*STAR SERC TSRP grant (#102 170 0137) and IMRE exploratory project fund (IMRE/14-1C0247).

Notes and references

1. (a) S. R. Forrest, *Nature*, 2004, **428**, 911-918; (b) S. I. Cho and S. B. Lee, *Accounts of Chemical Research*, 2008, **41**, 699-707; (c) A. Kros, R. J. M. Nolte and N. A. J. M. Sommerdijk, *Advanced Materials*, 2002, **14**, 1779-1782; (d) G. Schwartz, B. C. K. Tee, J. Mei, A. L. Appleton, D. H. Kim, H. Wang and Z. Bao, *Nat Commun*, 2013, **4**, 1859.
2. (a) H. N. Tsao, D. M. Cho, I. Park, M. R. Hansen, A. Mavrinskiy, D. Y. Yoon, R. Graf, W. Pisula, H. W. Spiess and K. Müllen, *Journal of the American Chemical Society*, 2011, **133**, 2605-2612; (b) H.-R. Tseng, L. Ying, B. B. Y. Hsu, L. A. Perez, C. J. Takacs, G. C. Bazan and A. J. Heeger, *Nano Letters*, 2012, **12**, 6353-6357; (c) R. D. McCullough and R. D. Lowe, *Journal of the Chemical Society, Chemical Communications*, 1992, 70-72.
3. (a) D. H. Kim, Y. Jang, Y. D. Park and K. Cho, *Langmuir*, 2005, **21**, 3203-3206; (b) B. Meredig, A. Salleo and R. Gee, *ACS Nano*, 2009, **3**, 2881-2886.
4. (a) H. Heil, T. Finnberg, N. von Malm, R. Schmechel and H. von Seggern, *Journal of Applied Physics*, 2003, **93**, 1636-1641; (b) C. Y. Yang, C. Soci, D. Moses and A. J. Heeger, *Synthetic Metals*, 2005, **155**, 639-642.
5. (a) L. Li, P. Gao, K. C. Schuermann, S. Ostendorp, W. Wang, C. Du, Y. Lei, H. Fuchs, L. D. Cola, K. Müllen and L. Chi, *Journal of the American Chemical Society*, 2010, **132**, 8807-8809; (b) W. Pisula, A. Menon, M. Stepputat, I. Lieberwirth, U. Kolb, A. Tracz, H. Sirringhaus, T. Pakula and K. Müllen, *Advanced Materials*, 2005, **17**, 684-689; (c) Y. Cao, Z. Wei, S. Liu, L. Gan, X. Guo, W. Xu, M. L. Steigerwald, Z. Liu and D. Zhu, *Angewandte Chemie International Edition*, 2010, **49**, 6319-6323.
6. (a) T. Lei, J.-H. Dou and J. Pei, *Advanced Materials*, 2012, **24**, 6457-6461; (b) J. Li, Y. Zhao, H. S. Tan, Y. Guo, C.-A. Di, G. Yu, Y. Liu, M. Lin, S. H. Lim, Y. Zhou, H. Su and B. S. Ong, *Sci. Rep.*, 2012, **2**.
7. (a) Y. Diao, B. C. K. Tee, G. Giri, J. Xu, D. H. Kim, H. A. Becerril, R. M. Stoltenberg, T. H. Lee, G. Xue, S. C. B. Mannsfeld and Z. Bao, *Nat Mater*, 2013, **12**, 665-671; (b) H. Minemawari, T. Yamada, H. Matsui, J. y. Tsutsumi, S. Haas, R. Chiba, R. Kumai and T. Hasegawa, *Nature*, 2011, **475**, 364-367.
8. C. Luo, A. K. K. Kyaw, L. A. Perez, S. Patel, M. Wang, B. Grimm, G. C. Bazan, E. J. Kramer and A. J. Heeger, *Nano Letters*, 2014, **14**, 2764-2771.
9. (a) R. R. Søndergaard, M. Hösel and F. C. Krebs, *Journal of Polymer Science Part B: Polymer Physics*, 2013, **51**, 16-34; (b) J. Chang, C. Chi, J. Zhang and J. Wu, *Advanced Materials*, 2013, **25**, 6442-6447.
10. D. Niedzialek, V. Lemaur, D. Dudenko, J. Shu, M. R. Hansen, J. W. Andreasen, W. Pisula, K. Müllen, J. Cornil and D. Beljonne, *Advanced Materials*, 2013, **25**, 1939-1947.
11. (a) I. Osaka, T. Abe, S. Shinamura and K. Takimiya, *Journal of the American Chemical Society*, 2011, **133**, 6852-6860; (b) S. Wang, M. Kappl, I. Liebewirth, M. Müller, K. Kirchhoff, W. Pisula and K. Müllen, *Advanced Materials*, 2012, **24**, 417-420.
12. H. Sirringhaus, *Advanced Materials*, 2014, **26**, 1319-1335